ISSN 2004-2965 Energy Proceedings, Vol. 22, 2021

International Conference on Applied Energy 2021
Nov. 29 - Dec. 5, 2021, Thailand/Virtual
Paper ID: 146

Topology Optimization of Liquid-cooled Heat Sinks with Different Inlets and Outlets

Yang Xia[1], Li Chen[1*], Ji-Wang Luo[1], Wen-Quan Tao[1]

1 Key Laboratory of Thermo-Fluid Science and Engineering of MOE, School of Energy and Power Engineering, Xi'an Jiaotong University, Xi'an, Shaanxi, P.R. China

ABSTRACT

With the increasing energy consumption of electronic equipment, heat sink design becomes a significant problem to be solved. Topology optimization for conjugated heat transfer problems in heat sinks has attracted numerous attention recently for its high degree of freedom in design. In this paper, liquid-cooled heat sinks with five different inlet and outlet structure combinations are optimized using bi-objective topology optimization based on the density method. The channel layouts in heat sinks are optimized and multiple optimal structures and corresponding Pareto frontlines are obtained. The results show that the well-distributed fluid can enhance the thermal performance of the heat sink. Heat sinks with inlets and outlets having natural distribution functions have better performance. It is also found that larger solid thermal conductivity can cause fewer winding channels.

Keywords: Topology optimization, density method, liquid-cooled heat sinks, bi-objective, conjugate heat transfer problem

1. INTRODUCTION

Liquid-cooled heat sinks including microchannel and minichannel heat sinks have attracted numerous attentions due to their tremendous potential in heat dissipation [1]. One of the most important factors that influences the thermal performance of liquid-cooled heat sinks is the layout of the channels [2, 3]. Liquid-cooled heat sinks with typical channels such as parallel straight channels, wavy channels and fractal channels have already been widely investigated [1, 2, 4]. However, such intuitive designs are probably not the optimal options for some certain problems [5].

Topology optimization is an effective numerical method to design heat sinks due to its high degree of freedom in design. It was first introduced by Bendsøe and Kikuchi [6] in 1988 to design mechanical structures under given loads, and was extended by Borrvall and Petersson [7] to fluid flow problems later in 2003. However, the results of topology optimization strongly depend on the geometric condition of inlet and outlet[8-10]. In the present study, heat sinks with five different inlet and outlet combinations are optimized using topology optimization based on density method and the superiority of different inlets and outlets are analyzed and evaluated in detail. Then the influence of the ratio of solid and fluid thermal conductivity is also investigated.

2. TOPOLOGY OPTIMIZATION OF HEAT SINKS

Here the 2D model of liquid-cooled heat sinks with different inlets and outlets are shown in Fig. 1. The heat sink consists of an inlet domain, a design domain and an outlet domain. For the inlet and outlet, five combinations named OC, TC, FC, SE and CE respectively are considered in this paper. In the design domain, the layout of embedded channels or the distribution of solid material is optimized using topology optimization to enhance the heat transfer and reduce the pressure drop of the heat sink. The design domain is discretized and for each element a design variable γ varying from 0 to 1 is assigned. γ=0 and γ=1 represent the solid phase and fluid phase, respectively.

2.1 Fluid dynamics modeling

Selection and peer-review under responsibility of the scientific committee of the 13th Int. Conf. on Applied Energy (ICAE2021).

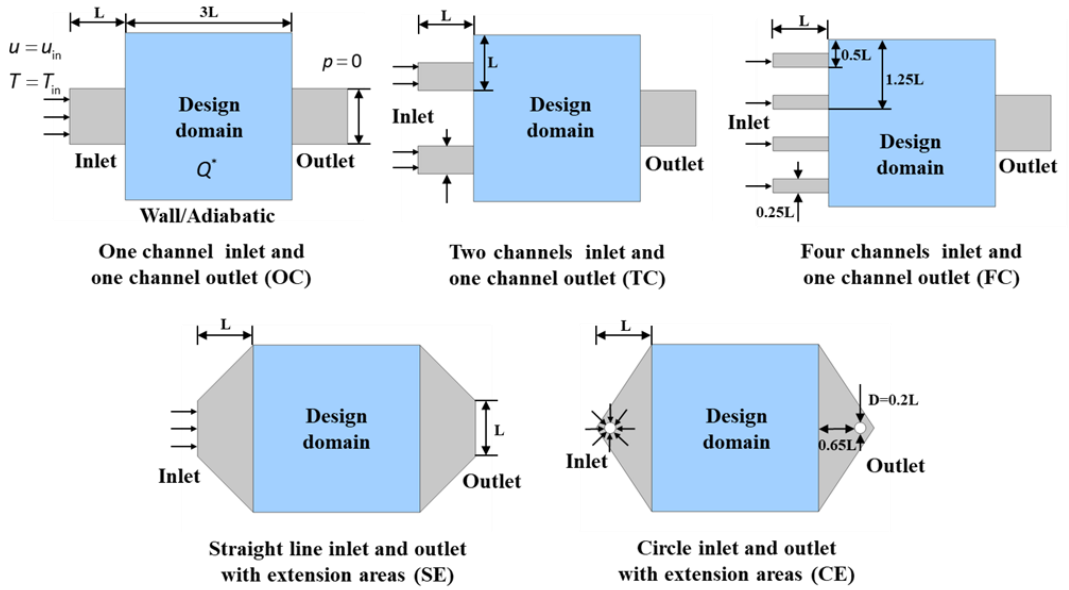

Fig. 1. The 2D model of liquid-cooled heat sinks with five different inlet and outlet combinations

For an internal flow problem, the incompressible steady-state Navier-Stokes equations in the non-dimensional forms are used as follows:

$$\nabla^* u^* = 0 \tag{1}$$

$$(u^* \cdot \nabla^*)u^* = \nabla^* \cdot [-p^* \mathrm{I} + \frac{1}{\mathrm{Re}}(\nabla^* u^* + (\nabla^* u^*)^{\mathrm{T}})] + F^* \tag{2}$$

where:

$$\nabla^* = L\nabla \quad u^* = \frac{u^*}{U} \quad p^* = \frac{p}{\rho U^2} \quad \mathrm{Re} = \frac{\rho UL}{\mu} \tag{3}$$

in which U is the inlet viscosity of fluid and L is the characteristic length. ρ and μ represent density and dynamic viscosity of fluid, respectively.

The dimensionless body force F^* in the Eq. (2) represents the flow resistance caused by the solid area as follows:

$$F^* = -\alpha^* u^* \tag{4}$$

where α^* is the dimensionless inverse permeability of the porous media dependent on the design variable γ [7]:

$$\alpha^* = \alpha^*_{\max} \frac{q(1-\gamma)}{1+\gamma} \tag{5}$$

in which q is the penalty parameter regulating the convexity of the interpolation function α^* and $\alpha^*_{\max}$ is determined by the Reynolds number and Darcy number as follows [11]:

$$\alpha^*_{\max} = (1 + \frac{1}{\mathrm{Re}})\frac{1}{Da} \tag{6}$$

The Darcy number needs to be small enough to ensure the velocity approaches zero in the solid domain. In the present work, $q=10^{-2}$ and $Da=10^{-4}$. The inlet boundary condition is uniform velocity and the outlet is constant pressure.

2.2 Heat transfer modeling

The non-dimensional energy equation is as follows:

$$\mathrm{RePr}(u^* \cdot \nabla^*)T^* = \nabla^{*2} T^* \text{ (in fluid domain)} \tag{7}$$

$$0 = K\nabla^{*2} T^* + Q^* \quad \text{(in solid domain)} \tag{8}$$

where:

$$T^* = \frac{T - T_{\mathrm{in}}}{T_{\mathrm{B}} - T_{\mathrm{in}}} \quad \mathrm{Pr} = \frac{\mu C_p}{k_{\mathrm{f}}} \quad K = \frac{k_{\mathrm{s}}}{k_{\mathrm{f}}} \tag{9}$$

T_{in} is the inlet temperature of fluid. T_{B} is another reference temperature or the base temperature. C_p, k_{f} and k_{s} represent specific heat, thermal conductivity of fluid and thermal conductivity of solid, respectively.

The heat source term Q^* in the Eq. (8) is an ideal dimensionless heat source which represents the heat exchange between the heat sink and a base plate in constant temperature T_{B} [12]:

$$Q^* = h^*(1 - T^*) \tag{10}$$

where h^* is the dimensionless parameter that represents the intensity of heat generation in the solid domain:

$$h^* = \frac{hL^2}{k_{\mathrm{f}}} \tag{11}$$

where h is the constant heat generation coefficient.

In topology optimization, the design variable γ can distinguish the solid domain and fluid domain. Thus Eq. (7) and Eq. (8) can be rewritten into one single equation by introducing the design variable γ as follows:

$$\gamma \mathrm{RePr}(u^* \cdot \nabla^*)T^* = ((1-\gamma)K + \gamma)\nabla^{*2} T^* + (1-\gamma)h^*(1 - T^*) \tag{12}$$

In the present work, the Prandtl number, Reynolds number and heat generation coefficient h* are set to

6.78, 100 and 100, respectively. The inlet temperature is set to 20℃.

2.3 Bi-objective topology optimization problems

For a liquid-cooled heat sink with channels embedded, the thermal-hydraulic characters, flow resistance and heat transfer performance, are most concerned. Thus, two objectives, including power dissipation [7] and total heat generation [12] are considered at the same time as follows:

$$J_{\mathrm{f}}=\int_{\Omega}[\frac{1}{\mathrm{Re}}\nabla^{*}u^{*}:(\nabla^{*}u^{*}+\nabla^{*}u^{*\mathrm{T}})+\alpha^{*}u^{*}\cdot u^{*}]\mathrm{d}\Omega \tag{13}$$

$$J_{\mathrm{th}}=\int_{\Omega}(1-\gamma)h^{*}(1-T^{*})\mathrm{d}\Omega \tag{14}$$

$$J=(1-\omega)\frac{J_{\mathrm{f}}}{J_{\mathrm{f},0.5}}-\omega\frac{J_{\mathrm{th}}}{J_{\mathrm{th},0.5}} \tag{15}$$

where ω is the weight factor of the thermal objective and Ω is the total volume of the heat sink. Due to the large magnitude difference between fluid objective and thermal objective, the normalization is applied by the objective calculation results of the 0.5 uniform initial design variable field. The upper bond of fluid volume fraction is set to 0.5 in this study.

In order to avoid checkerboard problems and alleviate mesh dependency, a Helmholtz density filter is used during the topology optimization [13]:

$$-r^{2}\nabla^{2}\gamma_{\mathrm{f}}+\gamma_{\mathrm{f}}=\gamma \tag{16}$$

where γ_{f} is the new design variable after filtration and r is the filter radius. In current study, r is set to 0.05L.

A hyperbolic tangent projection is also adopted to reduce the gray area and sharpen the boundary between solid and fluid [14]:

$$\gamma_{\mathrm{p}}=\frac{\tanh(\beta(\gamma_{\mathrm{f}}-\gamma_{\mathrm{c}}))+\tanh(\beta\gamma_{\mathrm{c}})}{\tanh(\beta(1-\gamma_{\mathrm{c}}))+\tanh(\beta\gamma_{\mathrm{c}})} \tag{17}$$

where γ_{p} is the new design variable after projection and β and γ_{c} are projection slope and critical point, respectively. In this paper, β and γ_{C} are set to 8 and 0.5, respectively.

In general, the topology optimization problem can be formulated as:

$$\text{Minimize}\quad J=(1-\omega)\frac{J_{\mathrm{f}}}{J_{\mathrm{f},0.5}}-\omega\frac{J_{\mathrm{th}}}{J_{\mathrm{th},0.5}}$$

$$s.t.\quad \int_{\Omega}\gamma\mathrm{d}\Omega\le 0.5V_{\Omega}$$

$$0\le\gamma\le 1$$

Eq. (1), (2), (12), (16) and (17)

2.4 Simulation methods

The equations above are solved by the Finite Element Method (FEM) and design variable field is updated by the sequential quadratic optimization solver SNOPT [15]. A uniform distribution of design variable with γ=0.5 is given as initial guess. The calculation will be terminated when the max residual of design variable is less than 10^{-6} or the iteration number exceeds 600.

3. RESULTS AND DISCUSSION

3.1 Topology optimization of heat sinks with five different inlet and outlet combinations

Five heat sinks with different inlet and outlet structure combinations are optimized. In each combination, the inlet velocity is adjusted to guarantee that the volume flow flux is the same for all the cases. K=1 is adopted here to get more bifurcated channel layouts [5]. The corresponding results are presented in Fig. 2. As shown in Fig. 2, with the increment of the weight of thermal objective, the channels are more winding and the temperature fields are more uniform due to the multiple sinuous channels cutting off solid regions. Furthermore, the maximum temperature also decreases. When the weight of thermal objective is equal to zero, which means minimizing the flow resistance only, the channel is much smoother and the fluid almost rushes to outlet straightly after flowing in the heat sink. For the results of the weight of thermal objective as unity, which means only thermal objective is considered, blocking is observed near the outlet. In such situation, the fluid will flow through the porous media and the pressure drop of the heat sink will be significantly high.

In Fig. 2, it is obvious that there are distribution structures and collection structures near the inlet and outlet in OC, TC and FC, leading to a well-distributed flow field. The channels near the inlet try to distribute fluid as uniform as possible, especially in results with large weight of thermal objective. However, similar structure is not observed in SE and CE. In order to further evaluate the performance of heat sinks with different inlet and outlet, the Pareto frontlines of five designs are plotted in Fig. 3. The design is more competitive if the Pareto frontline is closer to the top left corner. As can be seen from Fig. 3, the SE has better performance than OC, TC and FC due to natural distribution function of triangular extension area. There is no need for heat sinks with such inlet and outlet to design distribution structures which will cause more power dissipation. CE is also a common inlet and outlet structure. However, its performance is the worst at low weight of thermal objective but the best at high weight of thermal objective. This may be due to

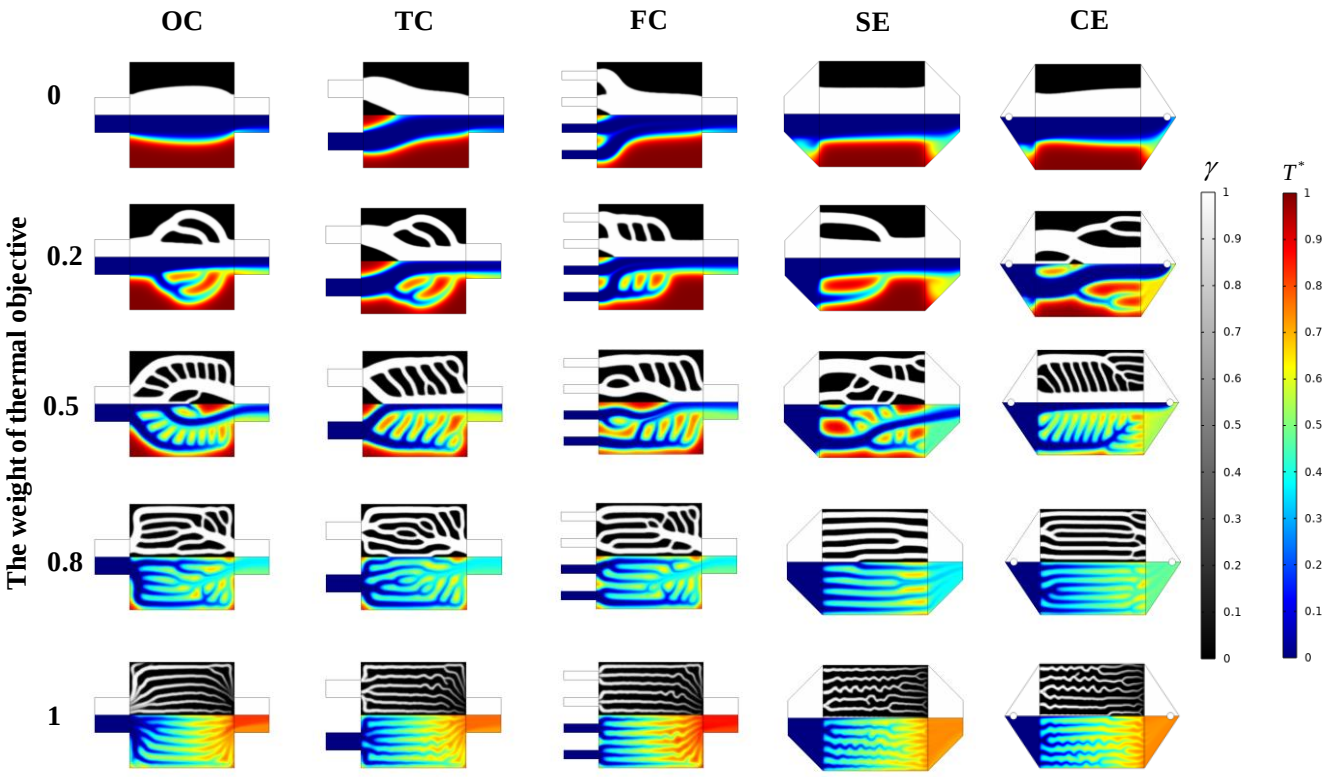

Fig. 2. The bi-objective topology optimization results of liquid-cooled heat sinks with five different inlet and outlet combinations

the inlet velocity is uniformly distributed on the circle. Some of fluid directly flow to the left boundary of the heat sinks, leading to more power dissipation. Such phenomenon can be more obvious at the low weight of thermal objective because of larger weight of fluid objective. While at the high weight of thermal objective, CE is better than SE due to its natural advantage of flow distribution attributed to circle inlet and outlet. It's worth mentioning that similar phenomenon can be observed in the reverse of Pareto frontlines of OC, TC and FC along with the increment of the weight of thermal objective in Fig. 3. It implies that better distribution ability does mean higher potential of thermal performance. However, some inlet and outlet structures may improve the distribution ability by means of sacrificing the flow resistance such as TC and FC, causing deterioration in fluid performance under high weight of fluid objective.

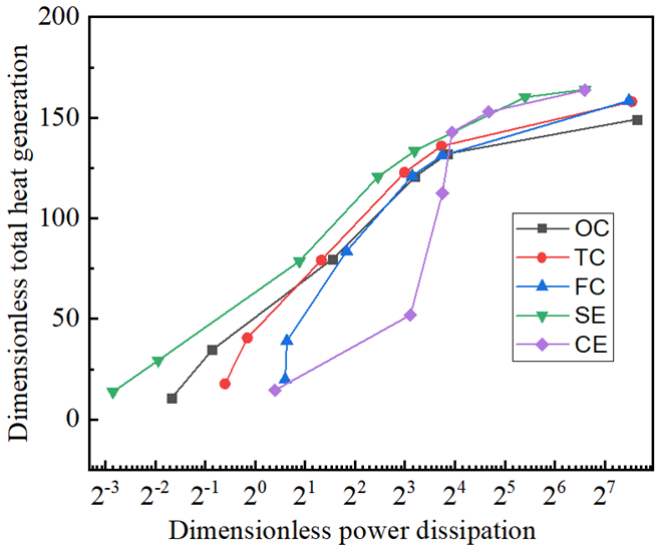

Fig. 3. The Pareto frontlines of five designs

3.2 The effect of the ratio of solid and fluid thermal conductivity

The effect of the ratio of solid and fluid thermal conductivity, *K*, is also investigated. Fig. 4 shows the optimization results for CE with different *K* when the weight of thermal objective is equal to 0.8. With the increase of the solid thermal conductivity, the channels are less winding, approaching the results at low weight of thermal objective. This is because large solid thermal conductivity means strong thermal diffusivity. For large solid blocks, the heat can be conducted to the solid-fluid boundary easily. There is no need to generate numerous winding channels cutting of the solid blocks to take away the heat. The fluid objective, the power dissipation, is the priority in such situation. Under such circumstance, the

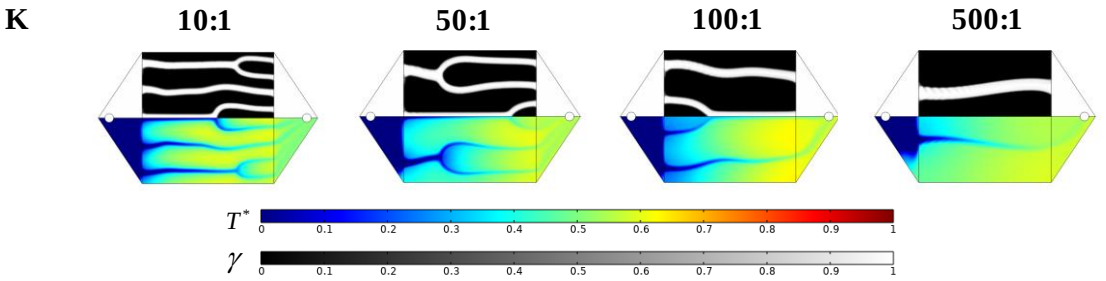

Fig. 4. The optimization results of CE with different K when ω=0.8

main thermal resistance is between the solid and fluid area. As a result, some fin structures begin to show up under large *K* to reduce the thermal resistance.

4. CONCLUSIONS

Liquid-cooled heat sinks with five different inlet and outlet structures are optimized using topology optimization based on the density method. Five Pareto frontlines and multiple novel designs are obtained. The main conclusions can be summarized as follows:

(1) The inlets and outlets influence the performance or potential of the heat sinks through their distribution ability. The well-distributed fluid can enhance the thermal performance of the heat sink.

(2) Better distribution ability of inlets and outlets is not bound to mean better performance. Although increasing the number of inlet channels can enhance the distribution ability, it will cause a reduction in flow performance under the low weight of thermal objective.

(3) The optimized layout of channels will be less winding along with the increment of the ratio of solid and fluid thermal conductivity.

ACKNOWLEDGEMENT

The authors thank the support of National Nature Science Foundation of China (51776159) and Shaanxi Province Science Fund for Distinguished Young Scholars (2019JC-01).

REFERENCE

[1] Dixit T, Ghosh I. Review of micro- and mini-channel heat sinks and heat exchangers for single phase fluids. Renewable & Sustainable Energy Reviews. 2015;41:1298-311.

[2] Sui Y, Teo CJ, Lee PS, Chew YT, Shu C. Fluid flow and heat transfer in wavy microchannels. International Journal of Heat and Mass Transfer. 2010;53:2760-72.

[3] Ghani IA, Sidik NAC, Kamaruzaman N. Hydrothermal performance of microchannel heat sink: The effect of channel design. International Journal of Heat and Mass Transfer. 2017;107:21-44.

[4] Wang XQ, Mujumdar AS, Yap C. Thermal characteristics of tree-shaped microchannel nets for cooling of a rectangular heat sink. International Journal of Thermal Sciences. 2006;45:1103-12.

[5] Li H, Ding XH, Meng FZ, Jing DL, Xiong M. Optimal design and thermal modelling for liquid-cooled heat sink based on multi-objective topology optimization: An experimental and numerical study. International Journal of Heat and Mass Transfer. 2019;144.

[6] Bendsoe MP, Kikuchi N. Generating optimal topologies in structural design using a homogenization method. Computer Methods in Applied Mechanics and Engineering. 1988;71:197-224.

[7] Borrvall T, Petersson J. Topology optimization of fluids in Stokes flow. International Journal for Numerical Methods in Fluids. 2003;41:77-107.

[8] Scholten T. A practical application of topology optimization for heat transfer and fluid dynamics. Dissertation, Delft University of Technology. 2017.

[9] Zhao X, Zhou MD, Sigmund O, Andreasen CS. A "poor man's approach" to topology optimization of cooling channels based on a Darcy flow model. International Journal of Heat and Mass Transfer. 2018;116:1108-23.

[10] Zhao JQ, Zhang M, Zhu Y, Cheng R, Li X, Wang LJ. Concurrent optimization of the internal flow channel, inlets, and outlets in forced convection heat sinks. Structural and Multidisciplinary Optimization. 2021;63:121-36.z

[11] Kondoh T, Matsumori T, Kawamoto A. Drag minimization and lift maximization in laminar flows via topology optimization employing simple objective function expressions based on body force integration. Structural and Multidisciplinary Optimization. 2012;45:693-701.

[12] Matsumori T, Kondoh T, Kawamoto A, Nomura T. Topology optimization for fluid-thermal interaction problems under constant input power. Structural and Multidisciplinary Optimization. 2013;47:571-81.

[13] Lazarov BS, Sigmund O. Filters in topology optimization based on Helmholtz-type differential

equations. International Journal for Numerical Methods in Engineering. 2011;86:765-81.
[14] Wang FW, Lazarov BS, Sigmund O. On projection methods, convergence and robust formulations in topology optimization. Structural and Multidisciplinary Optimization. 2011;43:767-84.
[15] Gill PE, Murray W, Saunders MA. SNOPT: An SQP algorithm for large-scale constrained optimization. Siam Journal on Optimization. 2002;12:979-1006.